(Article)

From amorphous to ordered: Structural transformation of Pd nanoclusters in 1-pentyne hydrogenation reactions

Kuo-Juei Hu [1,*], Peter R. Ellis [2], Christopher M. Brown [2], Peter T. Bishop [2], and Richard E. Palmer [3,*]

[1] National Laboratory of Solid State Microstructures, School of Physics, Nanjing University, Nanjing, 210093, China.; kuojueihu@nju.edu.cn
[2] Johnson Matthey Technology Centre, Blounts Court, Sonning Common, Reading, RG4 9NH, UK
[3] College of Engineering, Bay Campus, Swansea University, Fabian Way, Swansea, SA1 8EN, UK
[*] Correspondence: KJH: kuojueihu@nju.edu.cn; REP: r.e.palmer@swansea.ac.uk

Abstract: Nanostructured palladium catalysts are used industrially for selective alkyne hydrogenation reactions. However, structural changes can lead to a loss of performance. In this study, we show the evolution of the atomic structure of monodispersed Pd nanoclusters undergoing a vapour-phase 1-pentyne hydrogenation reaction. A specific structural transformation, from amorphous to highly symmetrical structures, is observed at the atomic level with aberration-corrected scanning transmission electron microscopy (AC-STEM). This surprising behaviour which occurs concurrently with the alkyne hydrogenation reaction, is clearly size-dependent. The results provide new understanding on the long-term stability of commercial heterogeneous catalysts.

Keywords: Mass-selected; Palladium nanoclusters; AC-STEM; Alkyne hydrogenation.

1. Introduction

The discovery of size-dependent quantum effects of ultra-small particles dates from the beginning of nanoscience. The evolution between discrete energy levels of individual atoms and the continuous energy bands of densely packed solids accounts for the novel properties of nanomaterials. In addition to particles' size, morphology affects some properties by defining facets and edges on the surface [1] as relevant to catalysis.[2] The modification of the particles during catalytic reaction is a key challenge for heterogeneous catalysis using metal nanoclusters. Even the migration of single atoms on the surface of the particles will lead to a change on morphology of the whole cluster. Thus the deterioration of catalytic performance (yield and/or selectivity) may develop with time under reaction conditions. In this context, the ability to produce size-selected metal nanoclusters with atomic precision is valuable in gaining an understanding of the structure change of a given particle size under reaction conditions. The morphology of such nanoparticles can be investigated with environmental transmission electron microscopy (ETEM).[3–6] However, intro-

ducing truly realistic reaction conditions while preventing damage by the intense electron beam as well as charged atom of the reaction is challenging.

Palladium is an effective catalyst for selective alkyne hydrogenation reactions.[7] The vapour-phase 1-pentyne hydrogenation reaction over Pd particles supported on Al_2O_3 has been shown to be mediated by a Pd-C complex .[8] Indeed, the hydrogenation events at the catalyst surface have been shown to be controlled by the incorporation of carbon and hydrogen into the surface. Pd hydride decompose above 353 K and PdC could accumulate onto the surface up to three atomic layers if the H_2/C_5 molar ratio is lower than 5. [9] However, Pd catalysts can also become deactivated by such processes.[10]

Size-selected Pd clusters have been proven to be good model systems for understanding the performance of real-life heterogeneous catalysts, in selective 1-pentyne hydrogenation amongst a number of reactions.[8,9,11–14] . Experimental [15] and theoretical[16] investigations of Pd clusters indicate that amorphous structures can be more stable than ordered icosahedral for certain sizes and temperatures. There is evidence of structural transformations towards a more stable Fcc and Dh structure could occur near the melting temperature. However, the reverse structural transformation from low configuration energy structures requires temperatures surpassing the melting point.[17] Hydrogen tends to diffuse into Pd particles, and the incorporation of hydrogen significantly lowers the melting point of Pd, on top of the melting point suppression due to the small size.[18,19] Structural transformations could proceed through a solid-liquid coexistence state, which could allow transformation to happen,[20] without the energy required to melt the whole cluster.

Mass-selected clusters provide several advantages in morphology studies given their uniform size and the relative ease of changing the nature of the clusters..[21] Further, the mass uniformity clarifies ripening phenomena. Historically, the mode and degree of ripening were tracked by measuring the log-normal distribution of particle size.[22] However, if ripening accompanies structural changes, identification of the structural transformations becomes difficult. A monodispersed selected size clusters onset is easier to trace.

Here, we report the structural evolution of atomic precision palladium nanoclusters supported on amorphous carbon films under realistic reaction conditions. We investigate the effect of 1-pentyne hydrogenation on the size and atomic structure of mass-selected $Pd_{923\pm20}$ and $Pd_{2057\pm45}$ clusters. This work builds on a preliminary study reported in

2014,[23] and that the new and more comprehensive study supersedes the preliminary study. Most significantly, by comparing with the previous work, we design experiments to distinguish heat treatment in hydrogen from exposure to the reaction. To establish what role the reaction itself plays in driving the restructure

The Pd clusters appear to be highly amorphous as prepared from the cluster beam source. The clusters of both sizes withstood annealing in inert gas without structural transformation to other structures. However, a transformation of Pd clusters to highly symmetrical cluster structures is triggered by 1-pentyne hydrogenation under the same annealing process. Cluster structures of all three high symmetries (FCC, Icosahedron, and Decahedron) were found to appear. Structural transformation in hydrogen-helium mixture of clusters of different size is observed. A considerable fraction of $Pd_{2057\pm45}$ clusters transformed to FCC and decahedral structure, but for $Pd_{923\pm20}$ the clusters remains amorphous.

2. Materials and Methods

Palladium nanoclusters were produced by a gas-phase condensation magnetron-sputtering cluster beam source. The lateral time-of-flight filter operating under a high vacuum regime (10^{-6}~10^{-7} mbar) was enclosed in a separate chamber attached to the source and set to provide the mass resolution of $M/\Delta M \approx 22$, based on calibration with Ar ion. The resulting size of Pd clusters made were 923±20 and 2057±45 atoms. The condensation length of formation is 250 mm for both size-selected clusters made. The size-selected nanoclusters were deposited directly onto standard amorphous carbon film (10 nm to 20 nm in thickness) supported by molybdenum TEM grids at the energy of 0.5 eV per atom. Nanoclusters were then brought to STEM (transferred through ambient conditions) for identification of their initial structure, within 7 days after the preparation. The samples were stored and transferred in a vacuum desiccator (~10^{-3} mbar) and the whole experiment was completed within 14 days. It is worth mention that the condensation length of Pd clusters in our preliminary study was 172 mm and the storage condition is 100 days in ambient.[24] This difference imply Pd clusters in this study are less oxidized and closer to its equilibrium state. The nanoclusters then underwent STEM imaging to probe the structural variation done by the treatment/reaction. The time for the nanoclusters to be exposed under ambient conditions throughout the whole process is less than 60 min altogether. Each of the TEM grids carrying nanoclusters is placed in the centre (on a quartz wool tube) of a quartz tube (length: 360 mm, inner diameter: 4 mm). For thermal annealing treatment, the gas flow of pure He (279 ml·min^{-1}) was used as an inert atmos-

phere. For the hydrogen reduction and the following 1-pentyne hydrogenation, the carrier gas is comprised of 40% H2/60% He (flow rate of 247 ml·min^{-1}). The reagent solution (1 M 1-pentyne plus 1 M 2-methylpentane (used as an internal standard for gas chromatography) dissolved in n-hexane) was introduced in the gas flow mentioned above through vaporising. The temperature was increased at a rate of 2 ℃/min from room temperature to 250 ℃ and then remained at the target temperature for 2 h. At the end of the reaction/treatment, cool He gas was flowed through the quartz tube for 30 min. STEM imaging was conducted with a JEOL-2100F operating at 200 keV equipped with a spherical aberration corrector (CEOS GmbH) and high-angle annular dark field (HAADF) detector. The inner and outer collecting angle of this detector were 62 and 164 mrad, respectively. Following imaging, the structure was identified by comparing the experimental images with the multi-slice image simulation over all possible orientation. Detail of assigning method is reported elsewhere.[2] Simulation images were generated using software package QSTEM.

3. Results and discussion

Our aim is to identify and distinguish the ripening and transformation of mass-selected Pd nanoclusters due to heat, hydrogen reduction, and the 1-pentyne catalytic hydrogenation reaction. Fig. 1(a) is a reference set of data observations of the Pd clusters before any chemical processing. It is observed from the images that the majority of the clusters lack order at atomic resolution. The corresponding FFT images shown in the rightmost column confirm that conclusion. The identification of high symmetry structures is illustrated by the result of hydrogenation of $Pd_{2057\pm45}$ shown in Fig. 1(b). The simulation atlas method is explained.[25–27] Atomic models that are used to generate simulated STEM images are shown on the side of the assigned experimental images, as in Fig 1(b)[24]

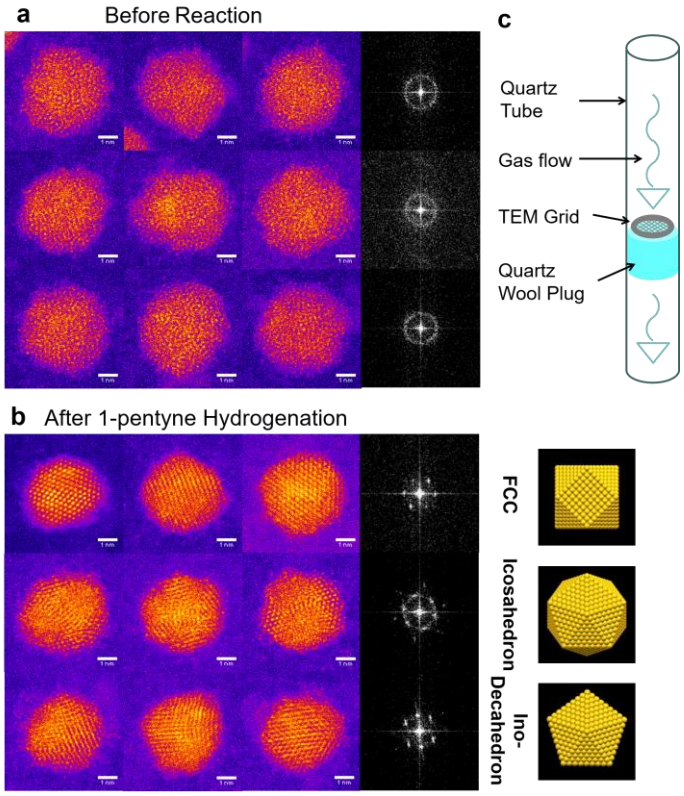

Figure 1. Panel is showing (a) atomic resolution representative images for $Pd_{2057\pm45}$ as prepared and (b) after a realistic 1-pentyne hydrogenation process as described in the experimental section. The converted FFT images of the rightmost experimental image in each row are shown. The images were taken by aberration-corrected HAADF-STEM with signal collected between 62 and 164 mrad. The scale bar located at the bottom right corner represented 1 nm in each cropped image. (c) Schematic of the realistic reaction processing setup.

The size distribution of $Pd_{923\pm20}$ nanoclusters before, Fig. 2(a), and after heat treatment in different atmospheres, Fig. 2(b) Helium, Fig. 2(c) Hydrogen/Helium, and Fig. 2(d) full 1-pentyne hydrogenation, were obtained. The main histogram from each condition was then divided into four rows, to display the populations of different isomer and amorphous structures under the same conditions, Fig. 2(e-h). The size distribution exhibits a single, sharp peak at 3.77±0.19 nm before reaction, Fig. 2(a). Almost all of the clusters produced are amorphous in the corresponding structural analysis, Fig. 2(e). Only a very small fraction of cluster is assigned to FCC and icosahedral isomers. Further, a shoulder in the size distribution indicates some degree of aggregation as the sample were prepared. The results from heat treatment in helium (2b, 2f) and a hydrogen-helium mixture (2c, 2g) show that in both treatments more aggregation occurs while all the clusters remain amorphous. The highest peaks in (2b, 2c) reflect the original cluster monomers, while the other peak at 4.78±0.16 nm indicates some degree of Smoluchowski ripening happens upon treatment. No obvious structural transformations due to heat treatment in helium or helium-hydrogen mixtures were observed. However, after a full 1-pentyne hydrogenation reaction, Fig. 2d, 2h, a considerable fraction of clusters was found to

transform to a high symmetry structure. For the original size clusters, the ratio between different structures is FCC:Ih:Dh:Amorphous is 3:2:2:9 after full 1-pentyne hydrogenation reaction. Similarly, for clusters which have aggregated from isomers, Fig. 2(h), the atomic structure is ordered in almost every one of them rather than remaining amorphous. Moreover, no matter what environment the $Pd_{923\pm20}$ were subjected to, no clusters were found to become smaller than their initial size, which indicates no disintegration of the $Pd_{923\pm20}$ due to the reaction.

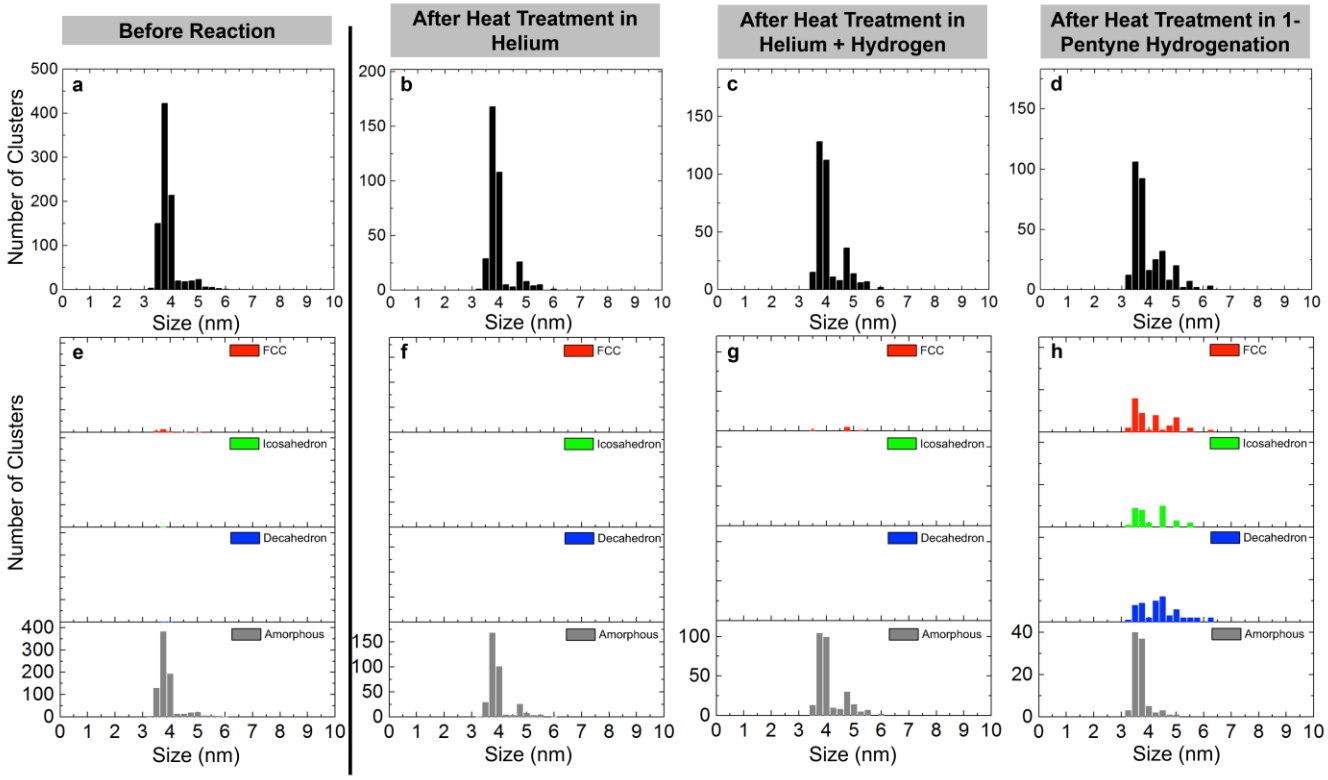

Figure 2: Charts showing the size distribution (a-d) and structural analysis with regards to size of clusters (e-h) of $Pd_{923\pm20}$ (a, e) before, after helium treatment (b, f), after helium hydrogen mixture (c, g) and after vapour-phase 1-pentyne hydrogenation treatment (d, h). The conditions for the thermal treatments were kept at 523 K for 2 h (ramp rate of 2 ℃/min from RT to ~250 ℃), under the atmosphere for helium treatment with gas flow of He (279 ml/min), for helium-hydrogen mixture with 40 % H_2 and 60 % He and the overall flow rate is 247 ml/min. For 1-pentyne hydrogenation, 1 M 1-pentyne in hexane was vaporised by carrier gas with flow rate identical as helium-hydrogen mixture. Independent pressure gauge and temperature sensor measured are 17.9~250.2 ℃; 0.30~0.34 bar (Helium treatment), 18.8~249.8 ℃; 0.20~0.23 bar (Helium/Hydrogen treatment), and 19.9~250.2 ℃; 0.32~0.35 bar (full 1-pentyne hydrogenation). Related cluster formation parameters: condensation length: 250 mm; magnetron sputtering power: 10 W DC; condensation pressure: 0.19~0.21 mbar; deposition energy: 0.5 eV/atom; condensation gas flows: 100 sccm (Ar) and 110 sccm (He).

A new peak arising from larger clusters emerged located at roughly 1.26 times of the size of the monomer indicating that these clusters are twice as the volume of a monomer. The ripening of size-selected clusters through the Smoluchowski model was discussed previously. Granqvist et al.[22] predicted a log-normal size distribution for Smoluchowski ripening of size-selected clusters.[28] Under Smoluchowski ripening conditions, the clusters should form discrete peaks (in mass), since all clusters are aggregates of the monomers. Although an under-investigated area,

amorphous structures have been observed in previous studies of Pd clusters larger than 1 nm.[15] The amorphisation process was investigated for various noble and quasi-noble metals,[16] in where amorphisation occurs by inserting more atoms into the five-fold symmetry corner on icosahedron. It was also found that this amorphisation process involved co-ordination numbers changing on the surface and in the interior of the cluster. A study on Pd_{55} clusters showed that amorphous structure is energetically more favourable over icosahedral when the temperature is above 600 K, which is higher than the temperature reached in this study. In our results, where the amorphous structure is often considered as metastable, we found it was still stable when simply heating the clusters in a helium atmosphere, which indicates that there is, at least, a considerable energy barrier between amorphous and high symmetry structures, if the later have lower energy.

Fig. 3 shows the size distribution 3(a-d) and structural analysis 3(e-h) of $Pd_{2057\pm45}$ clusters before reaction, after heating and hydrogen-helium atmospheres, and after the full 1-pentyne hydrogenation reaction. It can be seen that size distribution before reaction is comprised of a main peak (centre at 5.02±0.20 nm), the monomer, and a small dimer feature (centre at 6.34±0.29 nm) due to aggregation. The distribution remains the same after heat treatment in helium, with a slightly more obvious dimer feature at 6.3 nm. The structural analysis of both untreated 3(e) and heat-treated 3(f) clusters showed that the majority of clusters retain the amorphous structures. However, after the helium-hydrogen mixture treatment by contrast with the behaviour of $Pd_{923\pm20}$, a significant number of clusters transform into FCC and decahedral structures. The ratio of composition of the different structures within the monomer size region is (FCC:Ih:Dh:Amorphous) 8:2:10:9, Fig. 3 (g). In other words, more than two-thirds of the clusters have transformed into highly symmetrical structures. Among these, decahedral and FCC structure are the majority, with a few icosahedral. On the contrary, icosahedral is the highest proportion after 1-pentyne hydrogenation, Fig. 3(h), accounting for more than 40% of the monomer with high symmetry structures. Finally, there is no disintegration of the $Pd_{2057\pm45}$ clusters after treatment, which is similar to what is observed for $Pd_{923\pm20}$.

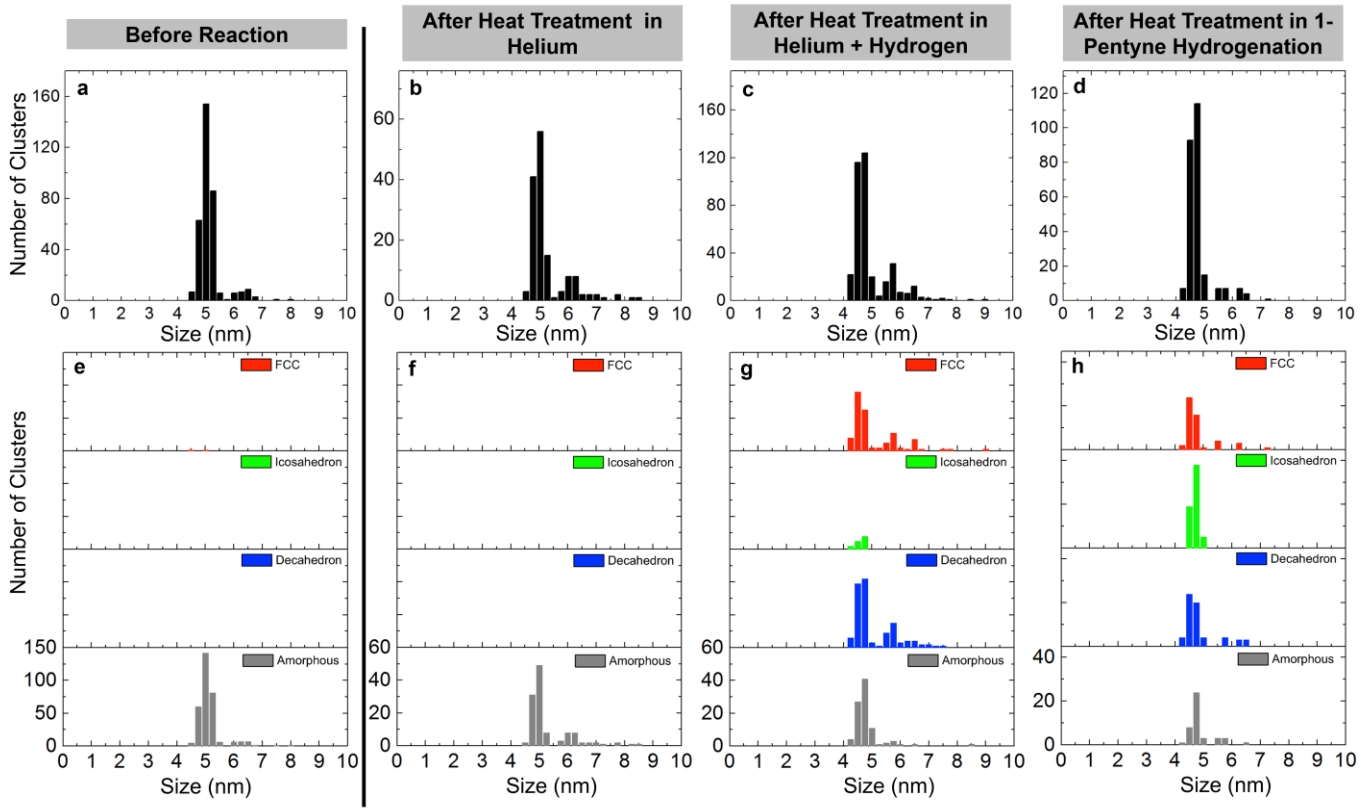

Figure 3: Charts show the size distribution (a-d) and structural analysis with regards to size of clusters (e-h) of $Pd_{2057\pm45}$ (a, e) before, after helium treatment (b, f), after helium hydrogen mixture (c, g) and after vapour-phase 1-pentyne hydrogenation treatment (d, h). The conditions for the thermal treatments were kept at 523 K for 2 h (ramp rate of 2 °C/min from RT to ~250 °C), under the atmosphere for helium treatment with gas flow of He (279 ml/min), for helium-hydrogen mixture with 40 % H_2 and 60 % He and the overall flow rate of 247 ml/min. For 1-pentyne hydrogenation, 1 M 1-pentyne in hexane was vaporised by carrier gas with flow rate identical as helium-hydrogen mixture. Independent pressure gauge and temperature sensor measured are 22.2~246.7 °C; 0.33~0.37 bar (Helium treatment), 19.4~247.8 °C; 0.22~0.25 bar (Helium/Hydrogen treatment), and 19.4~246.2 °C; 0.34~0.36 bar (full 1-pentyne hydrogenation). Related cluster formation parameters: condensation length: 250 mm; magnetron sputtering power: 10 W DC; condensation pressure: 0.19~0.21 mbar; deposition energy: 0.5 eV/atom; condensation gas flows: 100 sccm (Ar) and 110 sccm (He).

The survival of an amorphous structure for $Pd_{2057\pm45}$ after heat treatment in helium suggests once again that the local minimum in the potential energy surface is deep enough to stabilise amorphous structures for $Pd_{2057\pm45}$, as for $Pd_{923\pm20}$. Concerning Smoluchowski ripening, and assuming coalescence clusters are spherical,[29] the diameter of a dimer would be 1.26 times that of a monomer, and a trimer would be 1.45 times. Through curve fitting of the size distribution of treated samples, we found secondary peaks at 1.23 (5.70±0.17 nm) and 1.40 (6.46±0.16 nm) times the monomer peak (4.60±0.19 nm) after hydrogen treatment, and at 1.21 (5.63±0.07 nm) and 1.36 (6.36±0.07 nm) times the monomer peak (4.65±0.16 nm) after the 1-pentyne hydrogenation reaction.

In our reactions, the molar flow rate for H_2 and 1-pentyne are 4.41×10^{-3} moles/min and 6.00×10^{-5} moles/min, correspondently. The ratio of H_2/C_5 falls well within the region that H_2 is excessively supplied. Under this condition, it is considered that only a limit amount of PdC could build up.[8] Moreover, Fig. S1 confirms that there is little effect by post-treatment annealing in the atmosphere. This implies that the core structure of Pd clusters are not affected by the

oxidation even when it is inevitable. We argued that the structure identified in the TEM imaging is attributed to clusters' core structure. The surface oxidation layer needs to be removed in the reduction environment before allowing the cluster structure to transform.[30,31] This would also explain the stronger persistency of amorphous $Pd_{923\pm20}$ over $Pd_{2057\pm45}$ cluster in the hydrogen reduction environment since Pd clusters smaller than 3.7 nm have a higher oxidation saturation capacity.[32]

Structural transformations of the $Pd_{2057\pm45}$ clusters from amorphous to high symmetry structures were observed for both hydrogen and 1-pentyne hydrogenation treatments, but some subtle differences were noted. After treatment with hydrogen, few clusters transformed into icosahedral, whereas after full 1-pentyne hydrogenation, a significant number of icosahedral clusters emerged, alongside FCC, Dh, and amorphous structure were almost eliminated. This suggests that under hydrogen reduction environment, though little heat is generated, relieving of superficial oxide film by reduction liberates restructuring towards FCC and decahedron structures. In addition, under the combined effort of the exothermic release of heat and the presence of hydrogen, the intense reconstruction leaves only 15% of clusters staying amorphous after pentyne hydrogenation reaction. The extra heat of the exothermic hydrogenation reaction allows the clusters to convert from FCC and decahedron to access metastable icosahedron structures.[17] Heat release from semi-hydrogenation of the triple bond of 1-pentyne can be as high as 164.8-166 kJ/mol.[33–35] The turnover frequency per cluster of 3.6 nm in diameter is 1316 s^{-1} at 353 K, with 98 percent selectivity to double bond.[36] The heat produced in the catalytic reaction can then be estimated as $2.26\times10^{+3}$ $eV\cdot cluster^{-1}\cdot s^{-1}$. Moreover, the larger clusters would have higher turnover frequency due to their broader facet being more suitable for the organic molecule to bolt-on.[37] As a result, the reaction heat can induce structure transformation, and larger isomer clusters would generate more heat in the reaction, which makes them even more prone to structural conversion. It is noteworthy that, of these Pd clusters, which transformed from amorphous to icosahedral after the 1-pentyne hydrogenation reaction, none were dimers or trimers. This implies that the larger the size of the cluster, the larger the energy difference between the icosahedron and the other metastable high symmetry structures, FCC and decahedron.

4. Conclusions

In summary, we have distinguished between the effects of heat itself, thermal heating with hydrogen exposure, and thermal heating while the reaction is proceeding. In our aberration-corrected HAADF-STEM experiments, both $Pd_{923\pm20}$ and $Pd_{2057\pm45}$ amorphous clusters were found to transform to highly symmetrical structures after the full 1-pentyne hydrogenation reaction. FCC, decahedral and icosahedral clusters were all observed after the reaction. No such transformations were observed by heating the clusters in inert helium gas. This suggests that the exothermic reaction heat from the 1-pentyne hydrogenation may promote annealing of Pd nanoclusters while hydrogen's presence may relieving surface oxide and unlock transformation. The heat released from the triple-bond hydrogenation reaction will depend on the turnover frequency, which was reported[38] to peak at the size of our $Pd_{2057\pm45}$ clusters (5.0 nm). A size-dependent Pd cluster activity could also explain the observation that (a) hydrogen treatment at elevated temperature causes amorphous $Pd_{2057\pm45}$ clusters to transform into ordered isomers, whereas $Pd_{923\pm20}$ clusters remain amorphous, and (b) the proportion of icosahedral clusters structure produced by the full reaction is also found for $Pd_{2057\pm45}$ and $Pd_{923\pm20}$. In parallel with these observations, the cluster size distribution proceeds evolution for limited Smoluchowski ripening of the clusters under reaction conditions with no evolution for cluster disintegration (atom loss). It is believed that observation of both sintering and transformation of the atomic structure of clusters under reaction conditions will contribute to the optimisation of future nanocatalyst design.

5. Acknowledgement

The authors acknowledge EPSRC support, as well as the use of equipment funded through the Birmingham Science City project, 'Creating and Characterising Next Generation Advanced Materials,' supported by Advantage West Midlands (AWM) and part funded by the European Regional Development Fund (EDRF).

References

1. Lee, I.; Delbecq, F.; Morales, R.; Albiter, M.A.; Zaera, F. Tuning selectivity in catalysis by controlling particle shape. *Nat. Mater.* **2009**, *8*, 132–138, doi:10.1038/nmat2371.

2. Hu, K.-J.; Plant, S.R.; Ellis, P.R.; Brown, C.M.; Bishop, P.T.; Palmer, R.E. Atomic Resolution Observation of a Size-Dependent Change in the Ripening Modes of Mass-Selected Au Nanoclusters Involved in CO Oxidation. *J. Am. Chem. Soc.* **2015**, *137*, 15161–15168, doi:10.1021/jacs.5b08720.

3. Simonsen, S.B.; Chorkendorff, I.; Dahl, S.; Skoglundh, M.; Sehested, J.; Helveg, S. Ostwald ripening in a Pt/SiO2 model catalyst studied by in situ TEM. *J. Catal.* **2011**, *281*, 147–155, doi:10.1016/j.jcat.2011.04.011.

4. Simonsen, S.B.; Chorkendorff, I.; Dahl, S.; Skoglundh, M.; Sehested, J.; Helveg, S. Direct observations of oxygen-induced platinum nanoparticle ripening studied by in situ TEM. *J. Am. Chem. Soc.* **2010**, *132*, 7968–7975, doi:10.1021/ja910094r.

5. Challa, S.R.; Delariva, A.T.; Hansen, T.W.; Helveg, S.; Sehested, J.; Hansen, P.L.; Garzon, F.; Datye, A.K. Relating rates of catalyst sintering to the disappearance of individual nanoparticles during Ostwald ripening. *J. Am. Chem. Soc.* **2011**, *133*, 20672–20675, doi:10.1021/ja208324n.

6. Uchiyama, T.; Yoshida, H.; Kuwauchi, Y.; Ichikawa, S.; Shimada, S.; Haruta, M.; Takeda, S. Systematic morphology changes of gold nanoparticles supported on CeO 2 during Co oxidation. *Angew. Chemie - Int. Ed.* **2011**, *50*, 10157–10160, doi:10.1002/anie.201102487.

7. Cheung, T.-T.P.; Johnson, M.M. Catalyst and alkyne hydrogenation process. *NEW Eur. Pat.* **1996**, *2*.

8. Teschner, D.; Vass, E.; Havecker, M.; Zafeiratos, S.; Schnorch, P.; Sauer, H.; Knopgericke, a; Schlogl, R.; Chamam, M.; Wootsch, a Alkyne hydrogenation over Pd catalysts: A new paradigm. *J. Catal.* **2006**, *242*, 26–37, doi:10.1016/j.jcat.2006.05.030.

9. Teschner, D.; Borsodi, J.; Wootsch, A.; Révay, Z.; Hävecker, M.; Knop-Gericke, A.; Jackson, S.D.; Schlögl, R. The roles of subsurface carbon and hydrogen in palladium-catalyzed alkyne hydrogenation. *Science* **2008**, *320*, 86–89, doi:10.1126/science.1155200.

10. Albers, P.; Pietsch, J.; Parker, S.F. Poisoning and deactivation of palladium catalysts. *J. Mol. Catal. A Chem.* **2001**, *173*, 275–286, doi:10.1016/S1381-1169(01)00154-6.

11. Tew, M.W.; Nachtegaal, M.; Janousch, M.; Huthwelker, T.; van Bokhoven, J. a The irreversible formation of palladium carbide during hydrogenation of 1-pentyne over silica-supported palladium nanoparticles: in situ Pd K and L3 edge XAS. *Phys. Chem. Chem. Phys.* **2012**, *14*, 5761–8, doi:10.1039/c2cp24068h.

12. Habibpour, V.; Wang, Z.W.; Palmer, R.E.; Heiz, U. Size-◎Selected Metal Clusters: New Models for Catalysis with Atomic Precision. *ChemInform* **2012**, *11*, 1164–1170.

13. Tew, M.W.; Emerich, H.; van Bokhoven, J. a. Formation and Characterization of PdZn Alloy: A Very Selective Catalyst for Alkyne Semihydrogenation. *J. Phys. Chem. C* **2011**, *115*, 8457–8465, doi:10.1021/jp1103164.

14. Yin, F.; Lee, S.; Abdela, A.; Vajda, S.; Palmer, R.E. Communication: Suppression of sintering of size-selected Pd clusters under realistic reaction conditions for catalysis. *J. Chem. Phys.* **2011**, *134*, 141101, doi:10.1063/1.3575195.

15. José-Yacamán, M. High resolution TEM studies on palladium nanoparticles. *J. Mol. Catal. A Chem.* **2001**, *173*, 61–74, doi:10.1016/S1381-1169(01)00145-5.

16. Aprà, E.; Baletto, F.; Ferrando, R.; Fortunelli, a. Amorphization mechanism of icosahedral metal nanoclusters. *Phys. Rev. Lett.* **2004**, *93*, 10–13, doi:10.1103/PhysRevLett.93.065502.

17. Koga, K.; Ikeshoji, T.; Sugawara, K.I. Size- and Temperature-Dependent Structural Transitions in Gold Nanoparticles. *Phys. Rev. Lett.* **2004**, *92*, 2–5, doi:10.1103/PhysRevLett.92.115507.

18. Calvo, F.; Carré, a Structural transitions and stabilization of palladium nanoparticles upon hydrogenation. *Nanotechnology* **2006**, *17*, 1292–1299, doi:10.1088/0957-4484/17/5/022.

19. Grönbeck, H.; Tománek, D.; Kim, S.G.; Rosén, a. Does hydrogen pre-melt palladium clusters? *Chem. Phys. Lett.* **1997**, *264*, 39–43, doi:10.1016/S0009-2614(96)01293-6.

20. Schebarchov, D.; Hendy, S. Solid-liquid phase coexistence and structural transitions in palladium clusters. *Phys. Rev. B* **2006**, *73*, 121402, doi:10.1103/PhysRevB.73.121402.

21. Plant, S.R.; Cao, L.; Palmer, R.E. Atomic structure control of size-selected gold nanoclusters during formation. *J. Am. Chem. Soc.* **2014**, *136*, 7559–7562, doi:10.1021/ja502769v.

22. Granqvist, C.G.; Buhrman, R. a Size distributions for supported metal catalysts : Coalescence growth versus ostwald ripening. *J. Catal.* **1976**, *42*, 477–479, doi:10.1016/0021-9517(76)90125-1.

23. Hu, K.J.; Plant, S.R.; Ellis, P.R.; Brown, C.M.; Bishop, P.T.; Palmer, R.E. The effects of 1-pentyne hydrogenation on the atomic structures of size-selected AuN and PdN (N = 923 and 2057) nanoclusters. *Phys. Chem. Chem. Phys.* **2014**, *16*, 26631–26637, doi:10.1039/c4cp02686a.

24. Hu, K.-J.; Plant, S.R.; Ellis, P.R.; Brown, C.M.; Bishop, P.T.; Palmer, R.E. The effects of 1-pentyne hydrogenation on the atomic structures of size-selected Au N and Pd N (N = 923 and 2057) nanoclusters. *Phys. Chem. Chem. Phys.* **2014**, *16*, 26631–26637, doi:10.1039/C4CP02686A.

25. Batson, P.E.; Dellby, N.; Krivanek, O.L. Sub-ångstrom resolution using aberration corrected electron optics. *Nature* **2002**, *418*, 617–20, doi:10.1038/nature00972.

26. Nellist, P.D.; Pennycook, S.J. Direct Imaging of the Atomic Configuration of Ultradispersed Catalysts. *Science (80-.).* **1996**, *274*, 413–415, doi:10.1126/science.274.5286.413.

27. Yacaman, M.J. Structural instabilities in passivated gold nanoclusters induced by electron irradiation. *J. Clust. Sci.* **2002**, *13*, 189–197, doi:10.1023/A:1015543901226.

28. Fukamori, Y.; König, M.; Yoon, B.; Wang, B.; Esch, F.; Heiz, U.; Landman, U. Fundamental insight into the substrate-dependent ripening of monodisperse Clusters. *ChemCatChem* **2013**, *5*, 3330–3341, doi:10.1002/cctc.201300250.

29. Jensen, P. Growth of nanostructures by cluster deposition: Experiments and simple models. *Rev. Mod. Phys.* **1999**, *71*, 1695–1735, doi:10.1103/RevModPhys.71.1695.

30. Su, S.; Carstens, J.; Bell, A. A Study of the Dynamics of Pd Oxidation and PdO Reduction by H 2 and CH 4. *J. Catal.* **1998**, *176*, 125–135.

31. Kan, H.H.; Weaver, J.F. Mechanism of PdO thin film formation during the oxidation of Pd(111). *Surf. Sci.* **2009**, *603*, 2671–2682, doi:10.1016/j.susc.2009.06.023.

32. Schalow, T.; Brandt, B.; Starr, D.E.; Laurin, M.; Shaikhutdinov, S.K.; Schauermann, S.; Libuda, J.; Freund, H.J. Size-dependent oxidation mechanism of supported Pd nanoparticles. *Angew. Chemie - Int. Ed.* **2006**, *45*, 3693–3697, doi:10.1002/anie.200504253.

33. Rogers, D.W.; Dagdagan, O.A.; Allinger, N.L. Heats of Hydrogenation and Formation of Linear Alkynes and a Molecular Mechanics Interpretation. *J. Am. Chem. Soc.* **1979**, *101*, 671–676, doi:10.1021/ja00497a031.

34. Molnar, A.; Rachford, R.; Smith, G. V.; Liu, R. Heats of hydrogenation by a simple and rapid flow calorimetric method. *Appl. Catal.* **1984**, *9*, 219–223, doi:10.1016/0166-9834(84)80066-4.

35. Wagman, D.D.; Kilpatrick, J.E.; Pitzer, K.S.; Rossini, F.D. Heats, equilibrium constants, and free energies of formation of the acetylene hydrocarbons through the pentynes, to 1,500-degrees K. *J. Res. Natl. Bur. Stand. (1934).* **1945**, *35*, 467, doi:10.6028/jres.035.022.

36. Yarulin, A.; Yuranov, I.; Cárdenas-Lizana, F.; Abdulkin, P.; Kiwi-Minsker, L. Size-effect of Pd-(poly(N -vinyl-2-pyrrolidone)) nanocatalysts on selective hydrogenation of alkynols with different alkyl chains. *J. Phys. Chem. C* **2013**, *117*, 13424–13434, doi:10.1021/jp402258s.

37. Habibpour, V.; Song, M.Y.; Wang, Z.W.; Cookson, J.; Brown, C.M.; Bishop, P.T.; Palmer, R.E. Novel Powder-Supported Size-Selected Clusters for Heterogeneous Catalysis under Realistic Reaction Conditions. *J. Phys. Chem. C* **2012**, *116*, 26295–26299, doi:10.1021/jp306263f.

38. Crespo-Quesada, M.; Yarulin, A.; Jin, M.; Xia, Y.; Kiwi-Minsker, L. Structure sensitivity of alkynol hydrogenation on shape- and size-controlled palladium nanocrystals: Which sites are most active and selective? *J. Am. Chem. Soc.* **2011**, *133*, 12787–12794, doi:10.1021/ja204557m.

Supplementary material for

From amorphous to ordered: Structural transformation of Pd nanoclusters in 1-pentyne hydrogenation reactions

Kuo-Juei Hu [1,*], Peter R. Ellis [2], Christopher M. Brown [2], Peter T. Bishop [2], and Richard E. Palmer [3,*]

[1] National Laboratory of Solid State Microstructures, School of Physics, Nanjing University, Nanjing, 210093, China.; kuojueihu@nju.edu.cn
[2] Johnson Matthey Technology Centre, Blounts Court, Sonning Common, Reading, RG4 9NH, UK
[3] College of Engineering, Bay Campus, Swansea University, Fabian Way, Swansea, SA1 8EN, UK

S0.1 Further annealing in ambient conditions after heat treatment in helium/hydrogen mixture

Fig.S1 shows the composition of different structures of $Pd_{2057\pm45}$ nanoclusters before (Fig.S1 (a-b)) and after (Fig.S1 (c-d)) further annealing in ambient conditions after heat treatment in helium/hydrogen mixture. This independent experiment was conducted to investigate the degree of spontaneous oxidation of Pd clusters when they were exposed to the atmosphere. FCC was dominated by the structural population, as shown in Fig.S1 (b). The sample was then annealed in the ambient conditions under identical heat program (heat up (2 ℃/min from RT) and dwelled at 250 ℃ for 2 h). After the sample cooled down, the post-treatment STEM imaging was done immediately with a transferring time of less than 5 min. Results of the size distribution of $Pd_{2057\pm45}$ clusters showed the clusters did not suffer from serious ripening in Fig.S1 (c). Clusters did not aggregate into larger ones nor disintegrate into smaller fragments. Though a minute dimer peak was seen, clusters largely remain monomer. Fig.S1 (d) showed that the proportion of D_h increases slightly, and there emerged a tiny amount of I_h clusters. Nevertheless, in all cases, dominating high-symmetry structures remain.

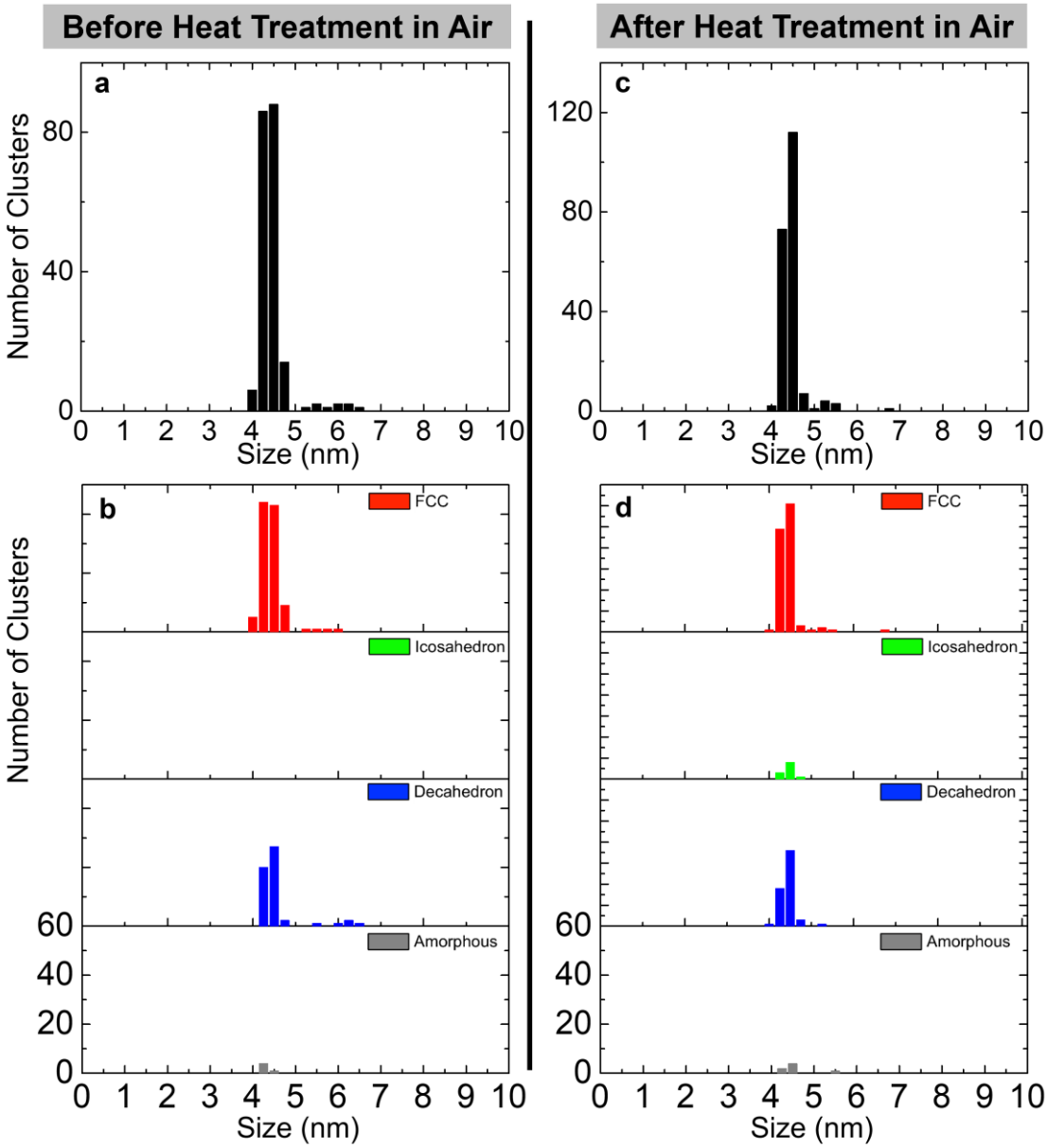

Figure S1 Charts (c,d) showing the relative population of further subsequent heat treatment in ambient condition, after heat-treated $Pd_{2057\pm45}$ in Helium/Hydrogen mixture (a,b). Four rows of histograms in (b) and (d) show the sub-distribution of clusters that are divided to three different structures identified. Heat treatment is done under ambient atmosphere and their temperature program is identical to other heat treatment in this study.